Modeling of Spectral Characteristics of the Links of Phase Distortions Autocompensator of Direct Digital Synthesizers

D. Surzhik[1], O. Kuzichkin[2], and G. Vasilyev[2,2(✉)]

[1] Vladimir State University, 23, St. Orlovskaya, Vladimir 602264, Russia
[2] Belgorod National Research University, 85, St. Pobedy, Belgorod 308015, Russia
vasilievgleb@yandex.ru

Abstract. The article presents a mathematical modeling of the spectral characteristics of the links of the path of generation of the control signal of the phase distortion autocompensator of digital computational synthesizers. The sources of distortion of the output signal of these devices are shown, which have a significant impact on their spectral purity and lead to undesirable phase modulation of the useful signal. The possibility of using automatic compensation to reduce the phase distortion of the output signal of direct digital synthesizers is considered. The functioning of the control signal generation of the autocompensator presupposes the isolation and processing of phase noise of the output signal. A model of the output signal of a direct digital synthesizer is obtained, taking into account parasitic phase modulation and distortions caused by truncation of the phase code, amplitude quantization and the nonlinearity of the converter from digital to analog form. The results of mathematical modeling confirm the effectiveness of the proposed algorithm for detecting phase impurities of the output signal of a direct digital synthesizer and reflect the functioning of the path forming the control signal of the phase distortion auto-compensator.

Keywords: Direct digital synthesizer · Automatic compensation · Spectral characteristics · Phase distortion

1 Introduction

Direct digital synthesizers (DDS) [1–8] are widely used as generators of stable frequencies and signals of various devices [9–16]. The block scheme of the DAC is represented in Fig. 1, where CLK is a clock generator, Acc is a phase accumulator, ROM is a read only memory device, DAC is a digital–to–analog converter, LPF is low-pass filter, K is the frequency code, f is the output frequency of the corresponding unit.

The important parameter of modern DDS is the spectral purity of the synthesized signal. In the process of frequency synthesis, the DDS output signal contains parasitic amplitude and phase distortions [7, 15–17]. The amplitude ones are characterized by a change in the ratio of the amplitudes of the components of the spectrum, and the phase ones lead to the fact that the DDS output signal contains a noise and a set of discrete

A. A. Radionov and V. R. Gasiyarov (Eds.): RusAutoCon 2023, LNEE 1130, pp. 166–173, 2024.
https://doi.org/10.1007/978-3-031-51127-1_16

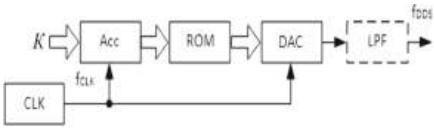

Fig. 1. The DDS block diagram.

harmful components, and their level can be significantly higher than that of indirect type synthesizers.

The greatest difficulty for suppression is the discrete components caused by the phase code truncation, the effect of destabilizing factors, and also the intrinsic noise of the DDS and quantization noise, since they are located in the near zone with respect to the synthesized oscillation and have a direct effect on its spectral purity. It is proved that these components lead to harmful deviations of the DAC output signal fronts: a change in their steepness and a time jitter. The process corresponds is similar to the parasitic phase modulation (PPM) of the useful signal, which makes it possible to consider their compensation to reduce the phase impurities of the DDS.

2 Adaptation of the Automatic Compensation Method in Relation to DDS

The main difficulty in the implementation of autocompensation is that the input and output DDS signals differ from each other in amplitude, shape and frequency, so it is complicated to compare them and isolate phase imputities [18–20]. Implementing the autocompensators of phase distortions (ACPD), a path for generation the DDS control signal has been developed and shown in Fig. 2a. The abbreviations represented in the scheme are: DC—differentiating circuit, Tr is trigger, FWR is full-wave rectifier, PD is phase detector, Amp is amplifier, DCD is delay control device, RP is reference path, IT is information path and CP is control path.

The functioning of the control signal formation of the autocompensator is the derivation and processing of phase impurities of the output signal. Finally, a control signal is formed, and further reduction of the DDS phase impurities is going on. The illustrative transient diagrams of the DDS ACPD is shown in Fig. 2b.

Figure 3 shows the DDS structures with ACPD implying forward (perturbation) and backward control (regulation by deviation). The double regulation scheme combines these two principles.

Figure 4 represents the normalized amplitude response of generators with APDS (Foffset is deviation from from the carrier frequency, and Fcut is cutoff frequency of the filter at the output of DDS). Transmission coefficient of DDS was set equal to 0.25.

As might be seen from Fig. 4, the described generators fully compensate the DDS signal impurities at small offset from the carrier oscillation, and partially suppress them at other frequencies. The most prominent suppression range is defined by the cutoff frequencies of the APDC low-pass filters.

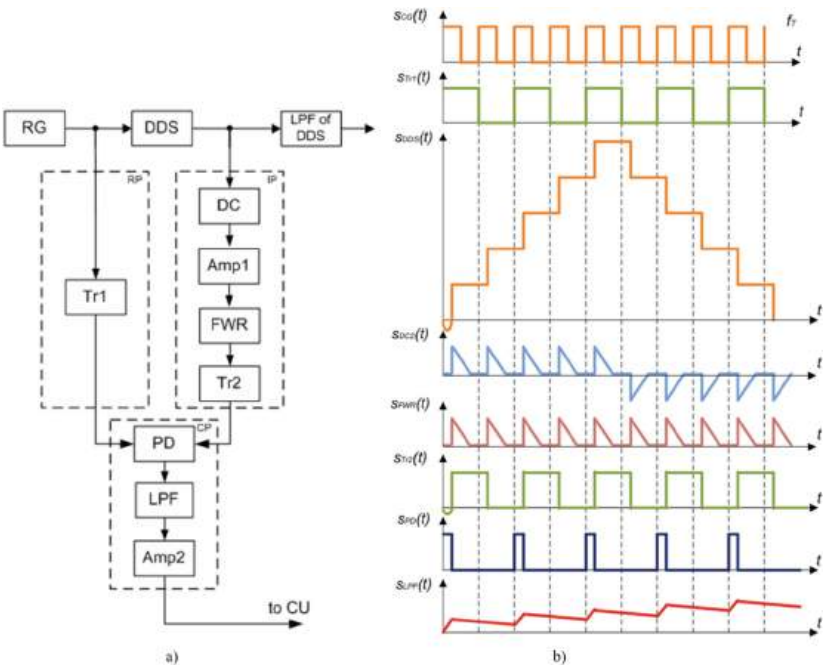

Fig. 2. Block scheme of the DDS control signal generation (**a**) and its transient diagrams (**b**).

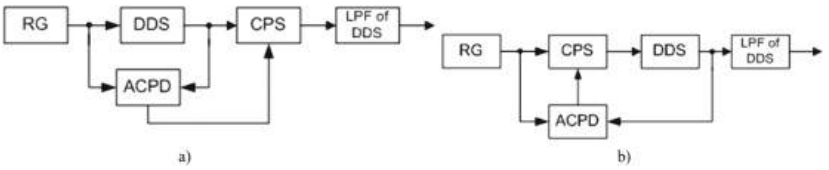

Fig. 3. Structures of the DDS with APDS and forward regulation (**a**) and backward regulation (**b**).

3 Mathematical Models of the DDS Output Signal

A model of the DDS output signal is known, which considers both distortions arising from phase truncation and distortions associated with quantization of the amplitude, defined by the expression

$$s_{DDS}(i) = \frac{trunc\left((N-1)\cdot sin\left(2\pi\frac{1}{2^a}trunc\left[mod\left[\frac{Kf_{CLK}}{2^p}t_i+\varphi_{ini},1\right]2^a\right]\right)\right)}{(N-1)} \quad (1)$$

where *trunc* (x) is the integer of x, $N = 2^n$ is the number of DAC quantization levels, n is the DAC bitrate, a is the ROM bitrate, $mod(x,y)$ is the remainder of the x/y division with the sign of x, $K = round\left(\frac{f_{CBS}M}{f_T}\right)$ is the output frequency code, *round* (x) is rounding to the closest integer, $M = 2^p$—the number of samples of the phase accumulator, p—the

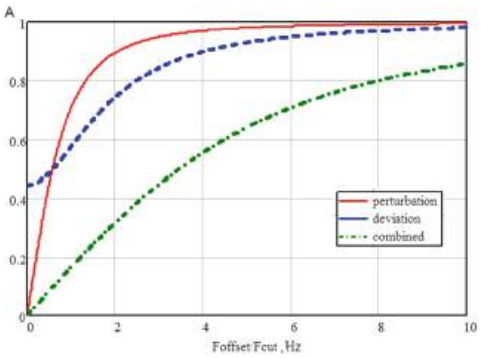

Fig. 4. Normalized amplitude response of DDS-based generators with APDC and various types of regulation.

capacity of the phase accumulator, $t_i = \frac{i}{f_{CLK}}$ are time samples, $i = 0\ldots M{-}1$, φ_{ini} is the initial phase.

However, this model does not take into account the real characteristic of the DAC conversion. An expression is obtained that allows to obtain the value of the analog output signal of a nonlinear DAC in units of voltage measurement

$$U_{DAC} = \Delta u\left(1 + \frac{Eg}{100\%}\right) \cdot \left(code + Di \cdot fi(code) + \frac{Dd}{4} fd(code) + E0\right) \quad (2)$$

where Δu is the scale factor of the conversion of the code into an analog signal, Eg—the gain error of the DAC, $code = -2^{n-1}\ldots 2^{n-1} - 1$—the digital code, Di—the amplitude of the integral nonlinearity function, c—the model of integral nonlinearity, Dd—the amplitude of the differential nonlinearity function, $fi(code)$ = rnd(1)—the model of differential nonlinearity, rnd(1)—the uniform distribution of the number in the range from 0 to 1, E_0—the error of the zero offset level.

4 Modeling of the Spectral Characteristics of the DDS Output Signal

Figure 5 shows the output signals of the information path links. Figure 6 represents the DDS output spectrum obtained by combining models (1) and (2), considering distortions caused by the phase code truncation, amplitude quantization and the DAC nonlinearity. The following device parameters were used for modeling: $f_{\text{CLK}} = 100$ MHz, $f_{\text{DDS}} = 4.993$ MHz, $K = 204$, $p = 12$, $a = 10$, $n = 14$, $\phi_{ini} = 0$, $Eg = 0.1$ LSB (least significant bit), $Di = 2$ LSB, $Dd = 1$ LSB, $E0 = 0.5$ LSB.

To simulate the phase distortion of the DDS output signal, we introduce the PFM into the model (1), replacing the initial phase with with a modulation law $s_{PPM}(i)$, which can be a purely sinusoidal, complex oscillation or a completely random process. Let's consider the simplest case—phase modulation by a harmonic signal

$$s_{PPM}(i) = \Delta\varphi_\varepsilon cos(2\pi f_\varepsilon t_i) \quad (3)$$

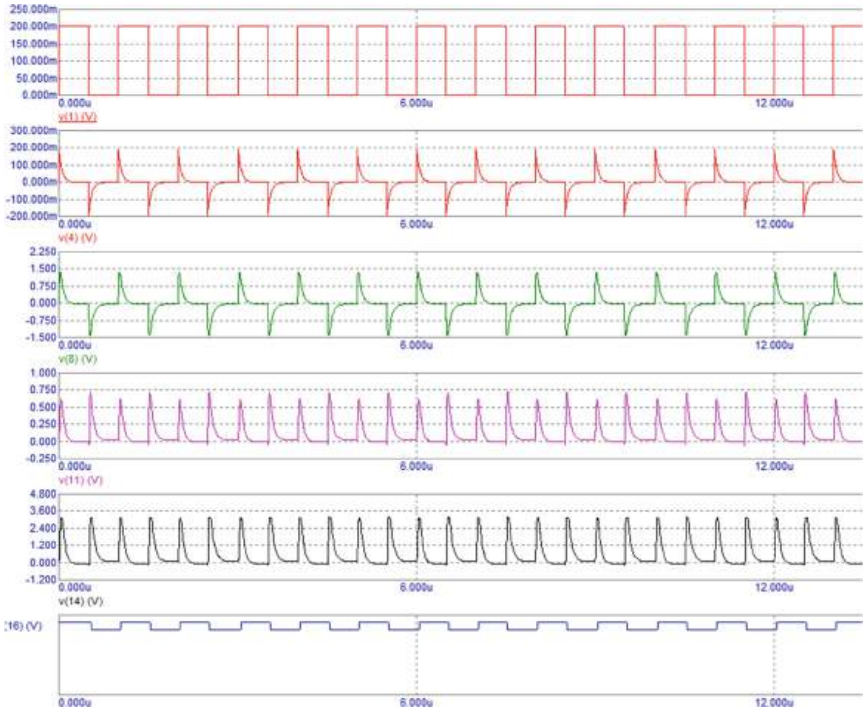

Fig. 5. Output transients of the information path links within the time range of 6 mcs (from above): a reference generator, a differentiating circuit, the first limiter amplifier, full-wave rectifier, the second amplifier and the second trigger.

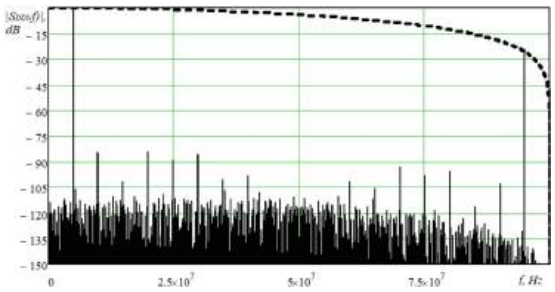

Fig. 6. The spectrum of the DDS output signal and its envelope.

Figure 7 shows the DAC output spectrum with PPM. For clarity of the results obtained, the following modulation parameters were adopted: modulation index $\Delta\varphi_\varepsilon =$ 0.1 rad, PPM frequency $f_\varepsilon = 2$ MHz.

Discrete harmful spectral components appear in the output signal, which significantly degrade the spectral quality of the output signal.

DC2 is used to separate the "steps" of the DAC output signal and to isolate the edges of the clock pulses with the PFM. As a result of the passage of a stepwise analog signal

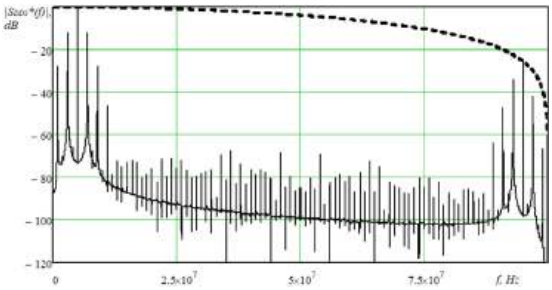

Fig. 7. The spectrum of the DDS output signal with PFM and its envelope.

through DC2, it is converted into alternating pulses of positive and negative polarity. In the frequency domain, this does not lead to a transformation of the phase composition of the spectrum, but only a redistribution of the amplitudes of the spectral components is observed—Fig. 8.

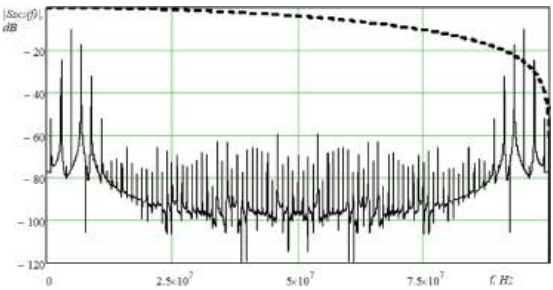

Fig. 8. The spectrum of the output signal of DC2 and the envelope of the output signal of the DDS DAC.

The full-wave rectifier of the information path converts the result of differentiation of the DAC step signal into a unipolar signal. Figure 9 shows the FWR output spectrum near the clock frequency.

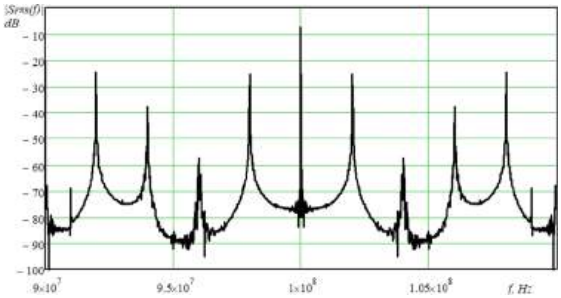

Fig. 9. Spectrum of the FWR output signal.

As a result of the nonlinear transformation, a 100 MHz component and PPM is present in the output of the FWR, and also even harmonics of the DDS output signal and their images with PPM.

In the frequency domain, the trigger Tr2 processing is similar to dividing the frequency of the input signal by 2 while preserving the PFM law—Fig. 10.

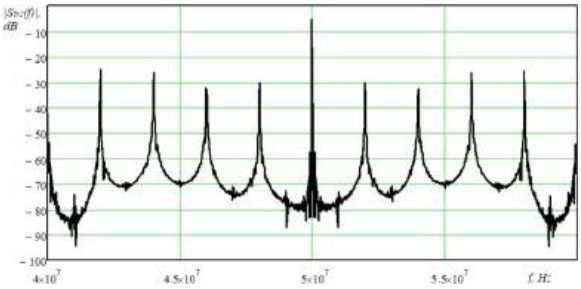

Fig. 10. The spectrum of the Tr2 output signal.

Subsequent processing of the reference and information signals is carried out in the control path of the ACPD. The phase detector PD compares the signals: a "pure" reference with a frequency of 50 MHz and information with the same frequency and PPM. Figure 11 represents the PD output spectrum within the range from 0 to 20 MHz.

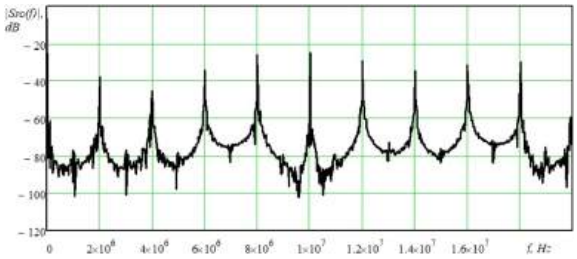

Fig. 11. Spectrum of the PD output signal.

As can be seen from the figure, there are spectral components in the spectrum with frequencies that are multiples of the PFM frequency.

5 Conclusion

Subsequent processing of the pulses allocated in the PD is performed by the low-pass filter isolating the constant component, and the amplifier Amp to level up the control signal.

The results of mathematical modeling confirm the effectiveness of the proposed algorithm for detecting phase impurities of the DDS output signal and reflect the functioning

of the path forming the control signal of the phase distortion autocompensator in the frequency domain.

Acknowledgments. The work was supported by the Scholarship of the President of the Russian Federation SP-4829.2021.3 "Increasing the quality indicators of modern space telecommunications systems by improving the characteristics of their radio transmitting equipment". The theory was prepared within the framework of the state task of the Russian Federation "Research and development of complex energy-saving and thermoelectric regenerative systems" application number 2019–1497, subject number FZWG–2020–0034.

References

1. Ridiko, L.: DDS: Direct digital frequency synthesis. Compon Technol, (7), (2001)
2. Yampurin, N.P.: Formation of precision frequencies and signals: textbook, p. 187. University, Nizhny Novgorod State Tech (2003)
3. Goldberg, B.G.: Digital frequency synthesis demystified, DDS and Fractional-N PLLs. Technology Publ., p 355 (1999)
4. Vankka, J., Halonen, K.: Direct digital synthesizers: theory, p. 208. Helsinki University of Technology, Design and Applications (2000)
5. Shakhtarin, B.I.: Frequency synthesizers: textbook. Hotline—Telecom, Moscow, p 128 (2007)
6. Kroupa, V.F.: Phase lock loops and frequency synthesis. John Wiley & Sons, Ltd, p 320 (2003)
7. Kester, U.: Analog-to-digital conversion, p. 1016. Technosphere, Moscow (2007)
8. Belov, L.A.: Formation of stable frequencies and signals: textbook for students higher. Studies. Institutions. Publishing center "Academy", Moscow, p 224 (2005)
9. Makarenko, V.: Synthesizers of the frequency of direct digital synthesis. Chipnews, (7), (2006)
10. Murphy, E.: All about DDS synthesizers. Compon Technol, (1), (2005)
11. Starikov, O.: Direct digital frequency synthesis and its application. Application News **3**, 56–64 (2002)
12. Anatychuk, L.I.: Thermoelements and thermoelectric devices. Kiev (1979)
13. Bernstein, A.S.: Thermoelectric generators. Gosenergoizdat, Moscow (1956)
14. Evdulov, O.V.: Development of devices and systems for cooling based on high-current thermoelectric energy converters. Dissertation for the degree of Doctor of Technical Sciences, Makhachkala (2019)
15. Kochemasov, V.: Digital computing synthesizers—modern solutions. Part 2. Electron: Sci, Technol, Bus **4**, 154–158 (2014)
16. Chenakin, A.: Frequency synthesis: current solutions and new trends. Electron: Sci, Technol, Bus, (1), (2008)
17. Makarychev, E.M.: Evaluation of the influence of nonlinear distortions of the digital and analog DDS path on the spectra of heterodyne signals in the field of Doppler detuning. Radio Engineering **4**, 105–111 (2015)
18. Surzhik, D.I., Kuzichkin, O.R., Vasilyev, G.S.: Development of a circuit design model of a signal generator of a payload of a UAV radio transmitter based on auto compensation of phase distortions. Int J Intell Syst Appl Eng **10**(3s), 118–122 (2022)
19. Surzhik, D.I., Kuzichkin, O.R., Vasilyev, G.S.: Development of a block diagram of a signal generator of a UAV radio transmitter based on auto compensation of phase distortions. Int J Intell Syst Appl Eng **10**(3s), 113–117 (2022)
20. Surzhik, D.I., Kuzichkin, O.R., Vasilyev, G.S.: Modeling of the payload signal generator of the UAV radio transmitter based on the phase distortion autocompensator. Int J Recent Innov Trends Comput Commun **10**(1), 15–18 (2022)